Acta Cryst. (1997). A53, 590–602

X-ray Scattering by Dislocations in Crystals. General Theory and Application to Screw Dislocations

L. E. LEVINE[a]* AND ROBB THOMSON[b]

[a]*School of Mechanical and Materials Engineering, Washington State University, Pullman, WA 99164-2920, USA, and* [b]*Materials Science and Engineering Laboratory, National Institute of Standards and Technology, Gaithersburg, MD 20899, USA. E-mail: lel@jeeves.nist.gov*

(Received 9 December 1996; accepted 18 April 1997)

Abstract

Line profiling of X-ray Bragg peaks has great potential for extracting meaningful physical parameters from work-hardened single-crystal samples; these include both dislocation densities and ordering lengths. However, a detailed reading of the existing literature uncovered shortcomings in the required theoretical understanding of scattering from dislocations. A mathematically rigorous theoretical framework is presented for understanding dislocation scattering; the procedure is based upon first principles of kinematic scattering and basic laws of probability theory. These results are then applied to the specific case of parallel screw dislocations. As expected from experimental measurements, the solution to this problem is neither Gaussian nor Lorentzian but is 'intermediate' between these distributions. Detailed computer simulations of the scattering are carried out and compared to the theoretical predictions. The predictions match the computer simulations with no adjustable parameters. Comparisons are also made to the work of previous authors.

1. Introduction

This paper is motivated by plans to study dislocation structure evolution in single-crystal metals deformed *in situ* at the National Synchrotron Light Source (NSLS) at Brookhaven National Laboratory. One of the principal techniques to be used will be line profiling of X-ray Bragg peaks (Mugrabi, Ungar, Kienle & Wilkens, 1986); to extract meaningful physical parameters from these data, a quantitative theoretical model is required. The theory of X-ray scattering of dislocations is an old subject, and the latest edition of a book by Krivoglaz (1996) serves as an excellent review of the previous work. Indeed, Krivoglaz, together with Wilkens (Wilkens, 1970*a*,*b*, 1984), has given the subject its current form.

Krivoglaz & Ryaboshapka (1963) examined scattering from an infinite cylindrical sample containing spatially uncorrelated screw dislocations with Burgers vectors parallel to the cylinder axis. Because of the symmetry of this system, we will refer to it as a two-dimensional (2D) dislocation distribution. In so far as it went, their analysis was essentially correct, showing that for small scattering vector, q, the distribution is well approximated by a Gaussian. Later, in his book, Krivoglaz (1996) predicts a simple power-law behavior at large q.

In a classic work, Wilkens (1970*a*) showed that in 2D, if a finite density of dislocations is embedded in an infinite lattice and if the total Burgers vector content of the infinite lattice is zero, then the energy per dislocation of the system is infinite. That is, the dislocation strain fields do not cancel over a distance of order equal to the average distance between dislocations. Because a physical arrangement of dislocations in a crystal cannot contribute a logarithmically divergent energy per dislocation, Wilkens introduced the concept of a 'restrictedly random' distribution. In this distribution, there exists a lattice block of finite size within which the dislocation total Burgers vector is zero; the physical crystal is composed of a set of such blocks of equal size containing equal total numbers of dislocations. Clearly, the energy per dislocation of the restrictedly random lattice is finite and proportional to the logarithm of the block size. Physically, the Wilkens postulate means that any very large crystal will eliminate the energy catastrophe by small rearrangements of its dislocations. In fact, it is thought that any deformed crystal will consist of low-energy dislocation structures for which the energy singularity is the driving force (Kuhlmann-Wilsdorf, 1995). Wilkens found that the same kind of logarithmic divergence appears in the scattering problem, and proposed the same construction for this case.

Unfortunately, owing in part to some apparent errors in one of Wilkens's papers (Wilkens, 1970*b*), we could not follow the details of his derivation (Wilkens, 1970*a*,*b*, 1984) and we were unable to reproduce physically correct line shapes for the scattering intensity from his solution for screw dislocations. Because of this difficulty, the only direct comparison we could make between the predictions of Wilkens and Krivoglaz was

in the asymptotic behavior of the scattering at large q. Unfortunately, Wilkens and Krivoglaz quote very different asymptotic behaviors. For all of these reasons, and because we must be able to interpret our own experimental results, we have developed, and report here, a new approach to the dislocation scattering problem, starting from first principles of kinematic X-ray scattering theory.

All physical dislocation distributions in crystals are three dimensional in the sense that the dislocations are almost never straight lines. However, 3D dislocation structures pose a major mathematical hurdle in nearly all cases and it is likely that a careful analysis of scattering from straight dislocations will still prove useful in analyzing real data. For these reasons, both Krivoglaz and Wilkens worked exclusively with straight dislocations and we follow their lead. From the point of view of scattering theory, it might ultimately be best to base the theory on the scattering of a collection of dislocation loops rather than on straight dislocations, and some work has been done along this line (Krivoglaz, 1996) but, for us, that approach will be reserved for the future.

In this paper, we present a general theoretical framework for dealing with the various problems of X-ray scattering from dislocations. This framework is very different from the approaches taken by Wilkens and Krivoglaz and has several distinct advantages. First, we believe our statistical approach is more mathematically rigorous than previous work in this field. Second, our analysis exhibits certain universality attributes reminiscent of the central limit theorem of probability theory. Thus, the expansion we use improves as the number of dislocations, N_d, increases; for large N_d, higher-order terms become completely negligible and only the first-order term is required to accurately predict the scattering distribution.

We next apply our general equations to the specific case of screw dislocations. The solution we obtain has a character intermediate between the Gaussian and Lorentzian forms, and is well approximated by a Voigt function (Young & Wiles, 1982). Although several similarities exist between our solution and those of Krivoglaz and Wilkens, significant differences also exist and are discussed. We do, however, confirm Wilkens's basic tenet, that the scattering of dislocated blocks scales with block size (at fixed dislocation density) such that the width of the scattering peak diverges logarithmically with block size. That is, large blocks lose their coherence. Thus, the observed peak profiles in any dislocation X-ray scattering experiment contain information on both the density (and type) of dislocations and the length scale over which ordering has taken place. This connects directly to the physical problem of what controls the dislocation patterning in a deforming crystal (Kuhlmann-Wilsdorf, 1995).

The theoretical structure of the dislocation scattering problem is very complex and requires several important approximations. This is true not only for us but for the other authors as well. Consequently, comparison between the various scattering models must be based upon computer simulations. We therefore include in this paper a rigorous and systematic comparison of the theoretical predictions with computer simulations of scattering from model systems. We find that our analytic treatment of the scattering problem beautifully matches the computer simulations, thus validating our theoretical results. Computer simulations will become even more essential for treating scattering from edge dislocations (work in progress) where many of our current approximations no longer apply.

The work reported here, and the work of Krivoglaz and Wilkens to which we primarily relate, is based on uniform random distributions of dislocations. The more recent work by Krivoglaz (1996) and Wilkens [Groma, Ungar & Wilkens (1988); Ungar, Groma & Wilkens (1989); see also Ungar & Borbeli (1996) for the most recent work] and their collaborators and a particularly important work by Gaal (1984) has dealt with the more difficult problem of the non-uniform correlations between the dislocations. Ultimately, one must confront the partially ordered problem. But our purpose here is to concentrate on the fundamental mathematical structure for dislocation scattering at its simplest level, where the analysis can be carried through with a minimum of approximation, and to compare it critically with computer simulations. After that has been accomplished, the more complicated problem of scattering from partially ordered dislocation structures can be addressed (perforce with significant additional approximations, and most desirably in 3D) in the light of appropriate computer simulations.

We stress that our goal is not merely to reproduce line shapes from dislocation arrangements. This could be accomplished using just the computer simulations. Instead, we require a quantitative theoretical model that describes the scattering in terms of the physical parameters we wish to explore. It is only through such a model that meaningful results can be extracted from experimental measurements.

In the next section, we present the general kinematical analysis, propose a way of introducing the dislocation statistics and show that this leads to a similar expansion of an exponential used by the previous authors. Detailed analyses of spatially uncorrelated screw dislocations in 2D are presented in §3 and the predicted shape is compared to the Gaussian and Lorentzian forms. Since nontrivial approximations are required for this analysis, in §4, we present computer simulations of scattering from dislocated lattices for comparison with the analytic predictions. This comparison is then used to validate the predictions for the screw case. §5 summarizes the paper and presents the

conclusions. Appendix *A* presents an asymptotic analysis for the tails of the scattering distribution that predicts a behavior distinct from the predictions of both Krivoglaz and Wilkens.

2. General kinematic scattering

We begin with the expression for the scattering intensity in the kinematic (single scattering, far field) limit given by (Warren, 1990; Krivoglaz, 1996)

$$I(\mathbf{q}) = S(\mathbf{q})S^*(\mathbf{q}), \tag{1}$$

where $\mathbf{q}$ is the scattering vector and $S(\mathbf{q})$ is the lattice structure factor,

$$\begin{aligned} S(\mathbf{q}) &= (1/N_0)\sum_{\mathbf{n}} \exp\{i\mathbf{q}\cdot\mathbf{r}(\mathbf{n})\} \\ &= (1/N_0)\sum_{\mathbf{n}} \exp\{i\mathbf{q}\cdot\mathbf{n}\}\exp\{i\mathbf{q}\cdot\mathbf{u}(\mathbf{n})\}, \end{aligned} \tag{2}$$

where N_0 is the number of atoms, $\mathbf{n}$ is a perfect lattice vector (we subsume in this sum any additional sums over the lattice basis), $\mathbf{r}(\mathbf{n})$ is the actual position of atom $\mathbf{n}$ and $\mathbf{u}(\mathbf{n})$ is the displacement at the lattice site caused by all of the dislocations in the crystal. In all of these equations, we have left out the atomic scattering factors, $f(\mathbf{q})$, which we take to be identical. Thus, our $I(\mathbf{q})$ must be multiplied by ff^* to obtain the absolute intensity. The normalization chosen relative to N_0 leads to $I(0) = 1$ for a perfect lattice, which simplifies the equations, but $N_0^2 I$ represents the actual intensity of scattering for a finite sample (relative to the incident intensity).

A central problem of dislocation scattering is how to deal with the sample size in the previous equation. We do this by adopting Wilkens's restrictedly random distribution construction; this also allows us to explore the block-size dependence of the scattering. Therefore, with him, we assume that the lattice is composed of a set (say M) of finite-sized blocks, each of the same size and shape, and each containing a random distribution of the same total number of dislocations, N_d. We assume that the scattering between the blocks is incoherent, which implies that the scattering intensity, I, of the total lattice is a sum of the scattering intensities of the individual blocks.

We will not assign any physical significance yet to these blocks, but, presumably, if a deformed crystal arranges its dislocations so that the energy per dislocation is finite, this arrangement will also destroy the scattering coherence between blocks.

With no approximations, $S(\mathbf{q})$ can be written as a sum over M blocks,

$$\begin{aligned} S(\mathbf{q}) &= (1/N_0)\sum_{\mathbf{m}} \exp\{i\mathbf{q}\cdot\mathbf{m}\}\sum_{\mathbf{l}} \exp\{i\mathbf{q}\cdot\mathbf{l}\} \\ &\quad\times \exp\{i\mathbf{q}\cdot\mathbf{u}(\mathbf{l}+\mathbf{m})\} \\ &= (1/N_0)\sum_{\mathbf{m}} \exp\{i\mathbf{q}\cdot\mathbf{m}\}\sum_{\mathbf{l}} \exp\{i\mathbf{q}\cdot\mathbf{l}\} \\ &\quad\times \exp\{i\mathbf{q}\cdot[\mathbf{u}^i(\mathbf{l}+\mathbf{m}) + \mathbf{u}^e(\mathbf{l}+\mathbf{m})]\}, \end{aligned} \tag{3}$$

where $\mathbf{l}$ is the ideal position of an atom in a block located at $\mathbf{m}$, $\mathbf{u}^i(\mathbf{l}+\mathbf{m})$ is the displacement due to dislocations internal to block $\mathbf{m}$ and $\mathbf{u}^e(\mathbf{l}+\mathbf{m})$ is the displacement due to dislocations external to the block.

In our first approximation, we replace the displacement from external dislocations with an average displacement field, $\mathbf{u}^e(\mathbf{l})$. An additional term must then be added to account for relative rotations and displacements of the block $\mathbf{m}$. Writing in just the displacement term, $d\mathbf{m}$, we obtain

$$\begin{aligned} S(\mathbf{q}) &= (1/N_0)\sum_{\mathbf{m}} \exp\{i\mathbf{q}\cdot(\mathbf{m}+d\mathbf{m})\}\sum_{\mathbf{l}} \exp\{i\mathbf{q}\cdot\mathbf{l}\} \\ &\quad\times \exp\{i\mathbf{q}\cdot[\mathbf{u}^i(\mathbf{l}+\mathbf{m}) + \mathbf{u}^e(\mathbf{l})]\}. \end{aligned} \tag{4}$$

Using the notation $\mathbf{m}^* = \mathbf{m} + d\mathbf{m}$ and substituting (4) into (1) gives

$$\begin{aligned} I(\mathbf{q}) &= (1/N_0^2)\sum_{\mathbf{m},\mathbf{m}'} \exp\{i\mathbf{q}\cdot[\mathbf{m}^* - \mathbf{m}'^*]\} \\ &\quad\times \sum_{\mathbf{l},\mathbf{l}'} \exp\{i\mathbf{q}\cdot[\mathbf{l}-\mathbf{l}']\}\exp\{i\mathbf{q}\cdot\mathbf{u}^e(\mathbf{l},\mathbf{l}')\} \\ &\quad\times \exp\{i\mathbf{q}\cdot\mathbf{u}^i(\mathbf{l}+\mathbf{m},\mathbf{l}'+\mathbf{m}')\}, \end{aligned} \tag{5}$$

where we define the difference of the displacements at sites $\mathbf{l}$ and $\mathbf{l}'$ as $\mathbf{u}(\mathbf{l},\mathbf{l}') = \mathbf{u}(\mathbf{l}) - \mathbf{u}(\mathbf{l}')$, with two lattice arguments.

Separating out the $\mathbf{m} = \mathbf{m}'$ terms then gives

$$\begin{aligned} I(\mathbf{q}) &= (1/N_0^2)\sum_{\mathbf{m},\mathbf{l},\mathbf{l}'} \exp\{i\mathbf{q}\cdot[\mathbf{l}-\mathbf{l}']\}\exp\{i\mathbf{q}\cdot\mathbf{u}^e(\mathbf{l},\mathbf{l}')\} \\ &\quad\times \exp\{i\mathbf{q}\cdot\mathbf{u}^i(\mathbf{l}+\mathbf{m},\mathbf{l}'+\mathbf{m})\} \\ &\quad+ (1/N_0^2)\sum_{\mathbf{m}\neq\mathbf{m}'} \exp\{i\mathbf{q}\cdot[\mathbf{m}^* - \mathbf{m}'^*]\} \\ &\quad\times \sum_{\mathbf{l},\mathbf{l}'} \exp\{i\mathbf{q}\cdot[\mathbf{l}-\mathbf{l}']\}\exp\{i\mathbf{q}\cdot\mathbf{u}^e(\mathbf{l},\mathbf{l}')\} \\ &\quad\times \exp\{i\mathbf{q}\cdot\mathbf{u}^i(\mathbf{l}+\mathbf{m},\mathbf{l}'+\mathbf{m}')\}. \end{aligned} \tag{6}$$

If the scattering from $\mathbf{m}^*$ and $\mathbf{m}'^*$ is (close to) incoherent as discussed above, then, with the assumption of the restrictedly random distribution, the second term in (6) becomes negligible and (6) can be rewritten as

$$\begin{aligned} \langle I(\mathbf{q})\rangle &= (M/N_0^2)\sum_{\mathbf{l},\mathbf{l}'} \exp\{i\mathbf{q}\cdot[\mathbf{l}-\mathbf{l}']\} \\ &\quad\times \exp\{i\mathbf{q}\cdot\mathbf{u}^e(\mathbf{l},\mathbf{l}')\}\langle A(\mathbf{l},\mathbf{l}',\mathbf{q};C)\rangle_C, \end{aligned} \tag{7}$$

where $\langle A\rangle$ will be called the amplitude function,

$$\langle A(\mathbf{l},\mathbf{l}',\mathbf{q};C)\rangle_C = \langle\exp\{i\mathbf{q}\cdot\mathbf{u}^i(\mathbf{l},\mathbf{l}';C)\}\rangle_C, \tag{8}$$

and the average is taken over all possible configurations, C, of dislocations. This approximation is only valid if the number of independent scattering blocks is large enough to adequately sample the set of dislocation configurations.

Equation (7) shows that the X-ray scattering intensity profile for the whole sample can be determined by the proper average over dislocation configurations within a

single block. The average over configurations can be rewritten as

$$\langle A(\mathbf{l}, \mathbf{l}', \mathbf{q}; C)\rangle_C = \sum_C P(C) \exp\{i\mathbf{q} \cdot \mathbf{u}^i(\mathbf{l}, \mathbf{l}'; C)\}, \quad (9)$$

where $P(C)$ is the probability of each dislocation configuration.

To this point, the only assumption we have made concerning the dislocation distribution is that the number of atoms and dislocations within each block is the same. We now invoke the 2D approximation alluded to in the *Introduction*, in which the dislocations are all parallel to the Z axis and the blocks are infinite in this direction. In this case, we only need to consider a 2D plane of atoms perpendicular to the Z axis. If the dislocations are uniformly distributed within a block as independent random variables, then

$$P(C) = P(\mathbf{t}_1)P(\mathbf{t}_2), \ldots, P(\mathbf{t}_{N_d}) = [1/N_R]^{N_d}, \quad (10)$$

where N_R is the number of sites in a block and $P(\mathbf{t})$ is the probability of finding a specific dislocation at a specific site $\mathbf{t}$.

We can then write the amplitude function as

$$\begin{aligned}\langle A(\mathbf{l}, \mathbf{l}', \mathbf{q}; C)\rangle_C &= [1/N_R]^{N_d} \sum_C \exp\{i\mathbf{q} \cdot \mathbf{u}(\mathbf{l}, \mathbf{l}'; C)\} \\ &= [1/N_R]^{N_d} \sum_C \prod_{\mathbf{d}_C} \exp\{i\mathbf{q} \cdot \delta(\mathbf{l}, \mathbf{l}'; \mathbf{d}_C)\} \\ &= [1/N_R]^{N_d} \left[\sum_{\mathbf{t}} \exp\{i\mathbf{q} \cdot \delta(\mathbf{l}, \mathbf{l}'; \mathbf{t})\}\right]^{N_d},\end{aligned} \quad (11)$$

where we have defined the variable $\delta(\mathbf{l}, \mathbf{l}'; \mathbf{d}_C)$ to denote the relative displacement at sites $\mathbf{l}$ and $\mathbf{l}'$ due to a single dislocation at $\mathbf{d}_C$ and N_d is the number of dislocations in the block. The sum over all lattice positions, $\mathbf{t}$, in (11) is the contribution to $\langle A\rangle$ from a single dislocation whose center is averaged over the lattice, and the power N_d simply means that the dislocation distribution is uncorrelated. Since the above probability distribution allows an unphysical superposition of dislocations on a single lattice site, this approximation is only valid for low dislocation densities (N_d/N_0) - an approximation that is always satisfied in reality. The highest dislocation density actually observed in cell walls is $N_d/N_0 \simeq 0.01$.

The external displacement term, $\mathbf{u}^e(\mathbf{l}, \mathbf{l}')$, is expected to be nearly constant over the area of an individual block, and becomes a constant phase factor in the analysis. We will simply assume $\exp\{\mathbf{u}^e(\mathbf{l}, \mathbf{l}')\} = 1$. Substituting (11) into (7) and rewriting as a double integral then gives

$$\langle I(\mathbf{q})\rangle = (1/V)^2 \int \exp\{i\mathbf{q} \cdot (\mathbf{l} - \mathbf{l}')\}\langle A(\mathbf{l}, \mathbf{l}', \mathbf{q}; C)\rangle_C \, d\mathbf{l} \, d\mathbf{l}'. \quad (12)$$

In this equation, we have set $M = 1$ since we are now considering the scattering from a single averaged block and V is the volume of a cylindrical block of radius L. Symmetry reduces the problem to 2D so the volume element becomes a circular cross section. The amplitude function then becomes

$$\begin{aligned}\langle A(\mathbf{l}, \mathbf{l}'\mathbf{q}; C)\rangle_C &= [\langle a(\mathbf{l}, \mathbf{l}', \mathbf{q})\rangle_{\mathbf{t}}]^{N_d} \\ \langle a(\mathbf{l}, \mathbf{l}', \mathbf{q})\rangle_{\mathbf{t}} &= (1/V) \int \exp\{i\mathbf{q} \cdot \delta(\mathbf{l}, \mathbf{l}'; \mathbf{t})\} \, d\mathbf{t}.\end{aligned} \quad (13)$$

Since $\langle a(\mathbf{l}, \mathbf{l}', \mathbf{q})\rangle_{\mathbf{t}}$ is raised to a high power, N_d, the maximum in the amplitude function will be converted into a strong and sharp peak. Our procedure, therefore, is to identify the peak in $\langle a(\mathbf{l}, \mathbf{l}', \mathbf{q})\rangle$ and then expand $\langle A(\mathbf{l}, \mathbf{l}', \mathbf{q})\rangle$ around this point.

For an arbitrary $\mathbf{l}$ and $\mathbf{l}'$, the relative displacement will be of order unity, so that the phase will vary from 0 to 2π as the integration over the dislocation position is carried out in (13). Thus, as the dislocation is varied from place to place in the block during the integration, the integrand will tend to cancel itself for typical choices for $\mathbf{l}$ and $\mathbf{l}'$, and the integral will be small compared to V. However, when the lattice sites are close together relative to the block size, L, the phase is close to zero for nearly all choices of dislocation position, and the integral approaches V. Thus, the maximum of the amplitude function is at $\mathbf{l} = \mathbf{l}'$ and the exponential can be expanded about zero phase. Indeed, because N_d is very large, the peak character will be captured accurately in the lowest-order expansion of the exponential. Similar expansions are often used in solving scattering problems but the usual justification involves displacement fields that decrease with distance; this is not true for dislocations where the displacement fields remain finite at infinity. The same expansion was also used by both Krivoglaz and Wilkens, although we believe their justifications for it were not rigorous for the above reason.

Because of the very high peak expected for the amplitude function, $\langle A\rangle$, it is convenient to write it as an exponential,

$$\begin{aligned}\langle A(\mathbf{l}, \mathbf{l}', \mathbf{q}; C)\rangle_C &= \exp(-T) \\ T &= -N_d \ln\langle a(\mathbf{l}, \mathbf{l}', \mathbf{q})\rangle_{\mathbf{t}}.\end{aligned} \quad (14)$$

The use of T corresponds to a cumulant expansion of the scattering (Krivoglaz, 1996).

The final expression in (11) can easily be generalized to handle dislocations of multiple types. For example, if we include $N_d^{\mathcal{A}}$ dislocations of type $\mathcal{A}$ and $N_d^{\mathcal{B}}$ dislocations of type $\mathcal{B}$, then

$$\begin{aligned}\langle A(\mathbf{l}, \mathbf{l}', \mathbf{q}; C)\rangle_{C_{\mathcal{A}}, C_{\mathcal{B}}} &= [1/N_0]^{N_d^{\mathcal{A}}} \left[\sum_{\mathbf{t}} \exp\{i\mathbf{q} \cdot \delta^{\mathcal{A}}(\mathbf{l}, \mathbf{l}'; \mathbf{t})\}\right]^{N_d^{\mathcal{A}}} \\ &\times [1/N_0]^{N_d^{\mathcal{B}}} \left[\sum_{\mathbf{t}} \exp\{i\mathbf{q} \cdot \delta^{\mathcal{B}}(\mathbf{l}, \mathbf{l}'; \mathbf{t})\}\right]^{N_d^{\mathcal{B}}}.\end{aligned} \quad (15)$$

One use of (15) would be to handle samples with several slip systems.

3. Application to screw dislocations

In this section, we will apply the procedures introduced in §2 to analyze the scattering from restrictedly random distributions of screw dislocations. We assume that the displacements are given by isotropic elastic theory, since anisotropic theory adds a degree of complexity that is not desired at this stage. Also, nonlinear core effects can be neglected, since the major issues in dislocation scattering revolve around what happens at large distances.

Two cases will be examined: (i) $B = \sum b_i = 0$ and (ii) $B = N_d$. In order to understand the difference between these two cases, consider the dislocations in pairs. In case (i), each pair will consist of a positive and a negative dislocation, while, for case (ii), both dislocations will have the same sign. Thus, for each pair, using (13) with the shorthand notation $p(\mathbf{t}) = \mathbf{q} \cdot \boldsymbol{\delta}(\mathbf{l}, \mathbf{l}'; \mathbf{t})$, we can write

$$\langle A^{(2)} \rangle = (1/V^2) \int \exp\{i[p(\mathbf{t}_1) \mp p(\mathbf{t}_2)]\}\, d\mathbf{t}_1\, d\mathbf{t}_2, \quad (16)$$

where the upper sign corresponds to $B = 0$ and the lower to $B \neq 0$. The imaginary part of this integral is

$$\begin{aligned} &\int \sin[p(\mathbf{t}_1) \mp p(\mathbf{t}_2)]\, d\mathbf{t}_1\, d\mathbf{t}_2 \\ &\quad = \int \sin[p(\mathbf{t}_1)] \cos[p(\mathbf{t}_2)]\, d\mathbf{t}_1\, d\mathbf{t}_2 \\ &\qquad \mp \int \sin[p(\mathbf{t}_2)] \cos[p(\mathbf{t}_1)]\, d\mathbf{t}_1\, d\mathbf{t}_2, \end{aligned} \quad (17)$$

which is zero for $B = 0$; when $B \neq 0$, the amplitude function is complex.

Since the scattering vector is very close to a Bragg condition, the phase factor in (13) can be written with a high degree of accuracy as $\mathbf{Q} \cdot \boldsymbol{\delta}(\mathbf{l}, \mathbf{l}'; \mathbf{t})$, where $\mathbf{Q}$ is the Bragg scattering vector (Warren, 1990). In the case of screw dislocations, both the Burgers vector and the dislocation line lie along the Z direction. Thus, $\mathbf{Q} \cdot \boldsymbol{\delta}(\mathbf{l}, \mathbf{l}'; \mathbf{t}) = Q_z \delta(\mathbf{l}, \mathbf{l}'; \mathbf{t})$, where $Q_z = 2\pi N_B / a_0$, a_0 is a lattice constant and N_B is the order of the Bragg reflection (along $\mathbf{Z}$). Thus, we see that reciprocal-lattice peaks will only be broadened if they have a component in the Z direction. Also, this broadening will be independent of both Q_x and Q_y.

In the following analysis, it will be important to refer frequently to Fig. 1, which shows the coordinate system together with the complicated collection of angle variables that describe the geometry of the screw dislocation problem. Substituting the isotropic approximation for displacement from a screw dislocation (Hirth & Lothe, 1982) in our geometry gives the phase factor as

$$\begin{aligned} &\mathbf{q} \cdot \boldsymbol{\delta}(\mathbf{l}, \mathbf{l}'; \mathbf{t}) = Q_z b\, \alpha(\mathbf{l}, \mathbf{l}'; \mathbf{t})/2\pi a_0 = N_B \alpha(\mathbf{l}, \mathbf{l}'; \mathbf{t}) \\ &\qquad \alpha \approx (d/r) \sin(\theta - \beta), \end{aligned} \quad (18)$$

where $\alpha(\mathbf{l}, \mathbf{l}'; \mathbf{t})$ is the relative angle between the dislocation at $\mathbf{t}$ and the two sites $\mathbf{l}$ and $\mathbf{l}'$ (see Fig. 1). In the above equation, we used the dipole term in a Taylor expansion for α and we took the Burgers vector to be a lattice vector, so $Q_z b/a_0 = 2\pi N_B$. We also introduced the variable $d = |\mathbf{l}' - \mathbf{l}|$, and the angles θ and β from the figure. The radius, r, is the distance between the dislocation and the point half way between $\mathbf{l}'$ and $\mathbf{l}$, $r = |\mathbf{t} - (\mathbf{l} + \mathbf{l}')/2|$.

Since the maximum value of the amplitude function occurs at $\mathbf{l} = \mathbf{l}'$ in the phase factor, expanding about this point gives, with reference to Fig. 1,

$$\begin{aligned} \langle a \rangle &= (1/V)\Big\{ \int d\mathbf{t} + iN_B \int \alpha\, d\mathbf{t} - [(N_B)^2/2] \\ &\qquad \times \int \alpha^2\, d\mathbf{t} + [(N_B)^4/24] \int \alpha^4\, d\mathbf{t} + \ldots \Big\} \\ &= 1 + i(N_B L d/V)\langle a_1 \rangle - [(N_B d)^2/2V]\langle a_2 \rangle \\ &\qquad + [(N_B d)^4/48VL^2]\langle a_4 \rangle + \ldots \\ \langle a_1 \rangle &= (1/L) \int [\sin(\theta - \beta)/r] r\, dr\, d\theta \\ \langle a_2 \rangle &= \int [\sin^2(\theta - \beta)/r^2] r\, dr\, d\theta \\ \langle a_4 \rangle &= 2L^2 \int [\sin^4(\theta - \beta)/r^4] r\, dr\, d\theta. \end{aligned} \quad (19)$$

The third-order term is not given because it is nonzero only for $B \neq 0$. Our treatment of the nonzero B case, given in §3.1, is only qualitative because of the difficult

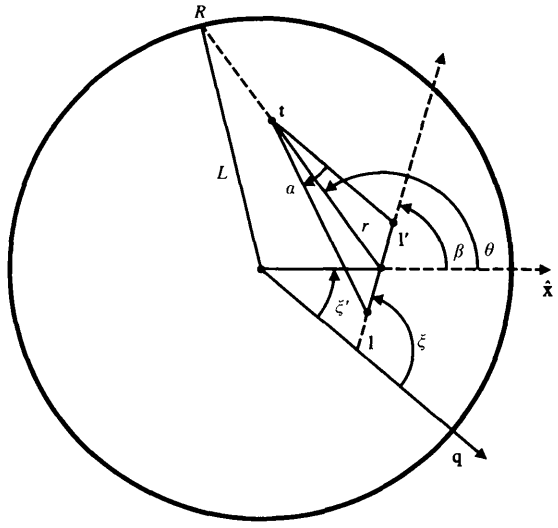

Fig. 1. The integration for the amplitude functions is over a circle of radius L. The origin for the integrations is not the center of the circle, it is placed at the center point of the vector joining the field points, $\mathbf{l}'$ and $\mathbf{l}$. From this origin, the distance to the dislocation at the point $\mathbf{t}$ is r and has a maximum value R. R is thus a function of the integration angle variable θ. The angle subtended by the two field points from the dislocation is called α. The angle between the x axis and the vector $\mathbf{l}' - \mathbf{l}$ is β. The scattering-vector direction is shown as $\mathbf{q}$ and the angle from this direction to the x axis is ξ'. The angle from the scattering vector to the vector $\mathbf{l}' - \mathbf{l}$ is ξ. The latter two angles are needed in the Fourier integrals for the scattering intensity.

analysis, so only the lowest-order (imaginary) term for $B \neq 0$ is needed.

The amplitude function can be evaluated by doing the integrations over the circle in Fig. 1, using as origin the center of the line between the field points, $\mathbf{l}$ and $\mathbf{l}'$. With the notation $l = |\mathbf{l} + \mathbf{l}'|/2$, the cosine law yields the relation $L^2 = R^2 + l^2 + 2lR\cos\theta$, from which the (normalized) upper integration limit for the radius, r, is $R/L = \rho(\theta) = -\lambda\cos\theta + (1 - \lambda^2\sin^2\theta)^{1/2}$, with $\lambda = l/L$. The lower limit is more subtle. For $r < d/2$, the dislocation lies within the circle defined by the field points, $\mathbf{l}$ and $\mathbf{l}'$, and the angle, α, is large. It will not then be correctly described by the dipole assumption in (18). Instead, when α is large, there should be no significant contribution to the integral. Thus, we take the lower limit to be $r_{\text{lower}} = d/2$ and the integrals become

$$\begin{aligned}\langle a_1\rangle &= (1/L)\int_0^{2\pi}\int_{d/2}^{R}[\sin(\theta-\beta)/r]r\,dr\,d\theta \\ &= \int_0^{2\pi}\sin(\theta-\beta)\rho\,d\theta \\ &= \cos\beta\int_0^{2\pi}\sin\theta[-\lambda\cos\theta + (1-\lambda^2\sin^2\theta)^{1/2}]\,d\theta \\ &\quad - \sin\beta\int_0^{2\pi}\cos\theta[-\lambda\cos\theta + (1-\lambda^2\sin^2\theta)^{1/2}]\,d\theta,\end{aligned} \tag{20}$$

from which

$$\langle a_1\rangle = \lambda\pi\sin\beta. \tag{21}$$

Further, with

$$\begin{aligned}\boldsymbol{\zeta} &= (\mathbf{l}' - \mathbf{l})/L; \quad \zeta = |\boldsymbol{\zeta}| \\ \boldsymbol{\lambda} &= (\mathbf{l}' + \mathbf{l})/2L; \quad \lambda = |\boldsymbol{\lambda}|,\end{aligned} \tag{22}$$

then

$$\begin{aligned}\langle a_2\rangle &= \int_0^{2\pi}\int_{\zeta/2}^{\rho}[\sin^2(\theta-\beta)/r]\,dr\,d\theta \\ &= \int_0^{2\pi}\sin 2(\theta-\beta)\ln(2\rho/\zeta)\,d\theta \\ &= \int_0^{2\pi}\cos^2\theta\ln(2\rho/\zeta)\,d\theta.\end{aligned} \tag{23}$$

This complicated integral can be evaluated exactly to give

$$\langle a_2\rangle = \pi\ln[(2/\zeta)(1-\lambda^2)^{1/2}]. \tag{24}$$

In a similar manner, the quartic integrals can be evaluated exactly to give

$$\langle a_4\rangle = (3\pi/\zeta^2) - [\pi/4(1-\lambda^2)^2][3 + \lambda^2(1+\sin^4\beta)]. \tag{25}$$

Numerical integration shows that the contribution of the λ variation to the overall results is minor for both $\langle a_2\rangle$ and $\langle a_4\rangle$, so we will use only the dominant term obtained in the limit $\lambda = 0$. We then get

$$\begin{aligned}\langle a\rangle &= 1 + iN_B\zeta\lambda\sin\beta + [(N_B\zeta)^2/2]\ln(\zeta/\zeta_0) + \cdots \\ \zeta_0 &= 2\exp(-N_B^2/8).\end{aligned} \tag{26}$$

The next step is the integration of the amplitude function to obtain the intensity from (12). When the total Burgers vector is zero, $B = 0$, the second term in (26) is zero, while, for $B = N_d$, all three terms must be used. We now carry out the quasi-Fourier sums over the amplitude functions to obtain the final intensity distribution for both of these two special cases.

3.1. *Zero total Burgers vector, B=0*

From (12),

$$\langle I(\mathbf{q})\rangle = (1/V)^2\int\exp\{i\mathbf{q}\cdot(\mathbf{l}' - \mathbf{l})\}\langle A\rangle\,d\mathbf{l}'\,d\mathbf{l}. \tag{27}$$

In developing this integration, first note that $\mathbf{Q}_z\cdot(\mathbf{l} - \mathbf{l}') = 2\pi N_B$, so only the deviation from the Bragg q vector $(\mathbf{q} - \mathbf{Q}_z)$ contributes. We note that $\langle A\rangle$ is not a function of l_z, so (27) is a δ function in z, and only the integration in the (X,Y) plane is considered; throughout the remainder of this paper, q will be expressed in units of $2\pi/a_0$. We will write $q = |\mathbf{q} - \mathbf{Q}_z|$ for a variable in this plane. With the variables ζ and λ, from (22), and the angle variables ξ and ξ' from Fig. 1, we can write the double volume (area) differential as $d\mathbf{l}\,d\mathbf{l}' = L^4\lambda\zeta\,d\zeta\,d\lambda\,d\xi\,d\xi'$. With this coordinate transformation, however, the limits are no longer simple. The limits on λ still go from 0 to 1 but the upper limit of ζ depends in a complicated way on the angle, much like the R variable in Fig. 1. Fortunately, the contribution to the ζ integration falls off very rapidly with increasing ζ, so the final solution to the scattering problem is insensitive to the upper limit, $\zeta_{\max}$. All that is required is to ensure that $\zeta_{\max}$ is small enough to satisfy the various approximations we have made. To illustrate the problem, we note that, if $\zeta > \zeta_0$ in (26), then the log term changes sign resulting in an unphysical divergence of the integral. Setting $\zeta_{\max} = \zeta_0/3$ completely solves this problem for all cases. Then, noting that $\langle A\rangle$ is not a function of λ for $B = 0$, and taking the first term in the expansion for $\ln\langle A\rangle$, we obtain the final solution

$$\langle I(q)\rangle = (L^4/V^2)\int\exp\{iq\zeta L\cos\xi\}\langle A(\zeta,\lambda)\rangle\zeta\lambda\,d\zeta\,d\lambda\,d\xi\,d\xi' \tag{28}$$

and

$$\begin{aligned}\langle I(q)\rangle &= 2\int_0^{\zeta_0/3}J_0(q\zeta L)\exp\{[-N_d(N_B\zeta)^2/2]\ln(\zeta_0/\zeta)\}\zeta\,d\zeta \\ \zeta_0 &= 2\exp(-N_B^2/8).\end{aligned} \tag{29}$$

J_0 refers to the zeroth-order Bessel function. Remember that the scalar, q, is the magnitude of the vector $|\mathbf{q} - \mathbf{Q}_z|$ in the (X,Y) plane. We will show in §4 that this solution beautifully matches our computer simulations, especially in the tails of the distribution.

The integration in (29) can only be performed numerically. First, we note that this function is definitely not a Gaussian. Fig. 2 shows a logarithmic plot of the predicted intensity as a function of q^2 (individual points). This plot exhibits a distinct curvature whereas a Gaussian would produce the straight line shown. This deviation from a Gaussian distribution is caused by the logarithmic ζ dependence in the exponential of (29). For completeness in Fig. 2, we also show a plot of a Lorentzian function fitted to the proper slope and starting value at $q = 0$ (upper curve).

The exponential term in (29) is essentially the Fourier–Bessel transform of the scattering function, $\langle I(q)\rangle$, and is the term Wilkens focuses on. He obtains the same prelogarithmic term we do in the exponential, but quite a different term from our logarithm (see Appendix 1 of Wilkens, 1970*a*). He claims (Wilkens, 1970*b*), however, that, in an approximation suitable for the physical case involved, the function he calls $f(\eta)$ reduces to a form similar to the logarithm given in our (29) [see equation (2.11) of Wilkens, 1970*b*]. The major difference is in how the Bragg order, N_B, enters into the two different expressions. Thus, in spite of very different mathematical approaches, we both come to similar (but distinct) predictions for the function we call $\langle A\rangle$. We note at this point that more serious differences exist in how we handle the measured intensity distributions, but we defer discussion of this point to the *Conclusions* section.

An important question involves the behavior of the scattering as a function of block size. We begin our investigation at the top of the scattering peak where $q = 0$. With the change of variable, $x = (\zeta/\zeta_0)^2$, (29) becomes

$$\langle I(0)\rangle = \zeta_0^2 \int_0^{1/9} x^{\eta x}\,dx$$
$$\eta = N_d N_B^2 \zeta_0^2/4 = N_d N_B^2 \exp(-N_B^2/8)/2. \tag{30}$$

Although the integrand has an essential singularity at the origin, the integral over this function is finite and well behaved. This integral can be estimated by assuming the Gaussian approximation of (29), which gives $x_d^{\eta x}$ instead of $x^{\eta x}$ in (30). Here, x_d is a constant that depends only upon N_d and N_B. This dependence can be determined by matching the values of these two functions at the point $1/\eta 2$, giving an optimized value of $x_d = \ln(2)/[\eta \ln(\eta)]$. We then obtain

$$N_0\langle I(0)\rangle = \langle I_a(0)\rangle \simeq 4/cN_B^2 \ln\{\eta \ln(\eta)/(\ln 2)\}, \tag{31}$$

where $\langle I_a\rangle$ is the scattering intensity per atom of the total sample and $c = N_d/N_0$ is the density of dislocations in the sample. This equation, with $N_B = 1$, is plotted along with a numerical evaluation of (30) in Fig. 3, which shows that (31) is an excellent approximation over the whole range of N_d explored. Larger values of N_d are unlikely to occur since this would imply unphysically large dislocation ordering distances.

Using the above value of x_d allows us to find the 'best fit' Gaussian approximation, $\langle I_G\rangle$, for (29),

$$\langle I_G(q)\rangle = 2\int_0^{\zeta_0/3} J_0(q\zeta L)\exp\{[-N_d(N_B\zeta)^2/4]\ln(1/x_d)\}\zeta\,d\zeta$$
$$= \{4/N_d N_B^2 \ln[\eta \ln(\eta)/(\ln 2)]\}$$
$$\times \exp\{-q^2L^2/N_d N_B^2 \ln[\eta \ln(\eta)/(\ln 2)]\}. \tag{32}$$

The functional form of (32) perfectly matches Krivoglaz's Gaussian prediction, but some of his parameters are different, thus leading to incorrect predictions of the scattering. For rough work, one can certainly approximate the scattering by a Gaussian. However, because the scattering deviates markedly from the Gaussian away from the peak, it will be

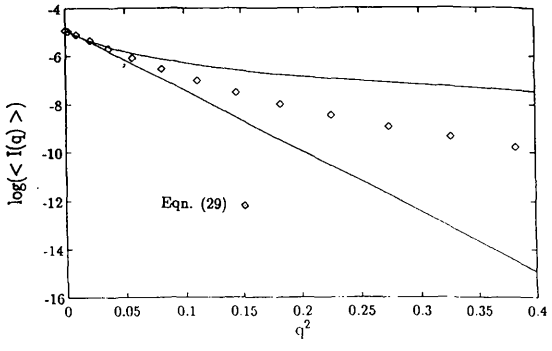

Fig. 2. Data points show $\ln\langle I(q)\rangle$ plotted as a function of q^2 using equation (29). For comparison, the figure shows Gaussian (straight line) and Lorentzian (curved line) curves fitted to the appropriate slope and value at $q = 0$. q is expressed in units of $2\pi/a_0$.

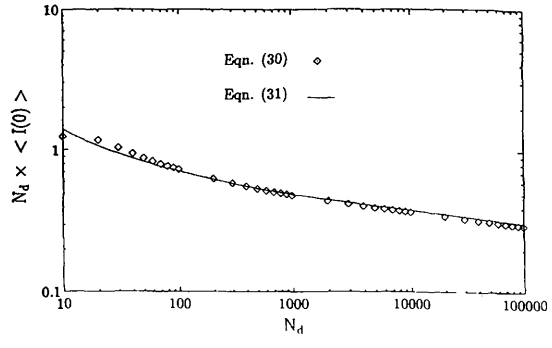

Fig. 3. Plot of $\langle I_a(0)\rangle$ *vs* the number of dislocations, N_d, for fixed dislocation density, c. The curved line is the approximate solution given by equation (31), while the points were obtained by numerical integration of equation (30).

important to use the correct shape in any interpretive use of scattering data.

Equation (31) shows that, for fixed c, $\langle I_a \rangle$ decreases logarithmically to zero as the sample size increases without limit. But since the integrated intensity per atom must be independent of the sample size, the decrease of the peak height to zero requires a corresponding divergence of the peak width. This is seen clearly in the Gaussian approximation, equation (32). The divergence of the peak width demonstrates that for a crystal with a fixed density of spatially uncorrelated dislocations, the scattering will become completely incoherent as the crystal size grows to infinity. This loss of scattering coherence should not be confused with problems of beam incoherence. What is happening physically is that the displacement fields of randomly distributed dislocations decrease the positional coherence of the atoms. Since the displacement field of a dislocation remains finite at infinite distance, the atomic coherence completely vanishes for infinite samples unless some ordering takes place to cancel these long-range displacement fields. The driving force for such ordering is the decrease in energy that occurs through this cancellation.

Observationally, one finds that dislocated crystals with moderate dislocation density retain distinct diffraction peaks. We conclude that this coherence arises from regions much smaller than the total sample size, in confirmation of the Wilkens (1970*a*) postulate.

Another important question concerns the asymptotic behavior of the scattering. Krivoglaz (1996) proposes a q^{-5} behavior of the scattering for large q, with a suggestion about how to derive it. However, following his hint, and after looking at our own analysis, we find a q^{-4} asymptotic relation for (29); the argument is presented in Appendix *A*. We also investigated this question by integrating (29) numerically and plotting the results; Fig. 4 is a logarithmic plot showing both the large-q behavior of this equation (points) and Krivoglaz's proposed q^{-5} behavior (straight line). Numerically, the scattering curve converges perfectly to Krivoglaz's prediction for the parameters given in the figure caption. By varying the parameters, N_d and L, however, we can obtain equally good agreement with our own q^{-4} prediction. This wandering behavior between q^{-4} and q^{-5} suggests that the behavior of (20) is more complicated than a simple power law for the range of q that we were able to explore numerically. At larger q, as proven in Appendix *A*, the behavior must ultimately approach q^{-4}. Finally, in both the computer simulations and our analytic work, we see no evidence for a power as low as q^{-3} as predicted by Wilkens (1970*b*). Comparison with experimental data is not appropriate at this stage since we have not yet included the effects of edge dislocations in the analysis.

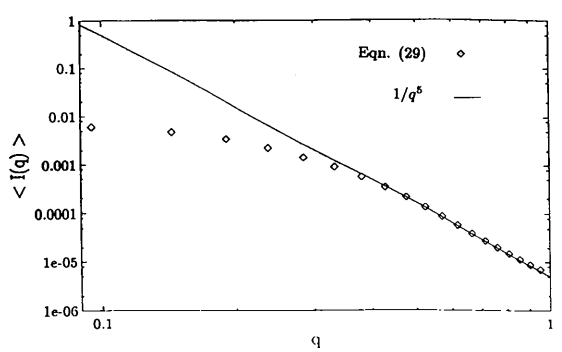

Fig. 4. ◇ log/log plot of equation (29), showing that in the extreme wings of the distribution, at least for a limited range of q, the scattering curve becomes power-like with a power in the range of −5, as suggested by Krivoglaz. The straight line shows a power function, $1/q^5$, for comparison. See text. q is expressed in units of $2\pi/a_0$

3.2. *Non-zero Burgers vector (the twisted crystal), $B \neq 0$*

The restrictedly random distribution was introduced to eliminate the problem of long-range strains in an infinite crystal. This rationale is not valid for the $B \neq 0$ case since the crystal would contain an infinite number of unpaired dislocations. However, as will be explained in §4, the averaging procedure we have introduced can also describe the scattering from a large (but finite) sample containing just one block. We will therefore continue our analysis of the $B \neq 0$ case using the same techniques as used for the $B = 0$ case.

When $B \neq 0$, the first three terms in the expansion of $\langle a \rangle$ in (26) are taken. As before, substituting this equation into (12) and using the T expansion of (14) leads to

$$\begin{aligned}\langle I(q)\rangle &= (1/\pi^2)\int \exp\{i\zeta[qL\cos\zeta + N_dN_B\lambda\sin(\zeta-\zeta')]\}\\ &\quad\times\exp\{-[N_d(N_B\zeta)^2/2]\ln(\zeta_0/\zeta)\}\zeta\lambda\,d\zeta\,d\lambda\,d\xi\,d\xi'\\ &= (1/\pi^2)\int \exp\{i\zeta h\sin(\xi+\chi)\}\\ &\quad\times\exp\{-[N_d(N_B\zeta)^2/2]\ln(\zeta_0/\zeta)\}\zeta\lambda\,d\zeta\,d\lambda\,d\xi\,d\xi'\\ &= (2/\pi)\int J_0(h\zeta)\exp\{[N_d(N_B\zeta)^2/2]\\ &\quad\times\ln(\zeta/\zeta_0)\}\zeta\lambda\,d\zeta\,d\lambda\,d\xi'\\ &\simeq \{4/\pi N_dN_B^2\ln[\eta\ln(\eta)/(\ln 2)]\}\\ &\quad\times\int_0^{2\pi}\int_0^1 \exp\left(-\{h^2/N_dN_B^2\ln[\eta\ln(\eta)/(\ln 2)]\}\right)\\ &\quad\times\lambda\,d\lambda\,d\xi'. \end{aligned} \tag{33}$$

In expanding the various sinusoidal functions in these integrations, we have used the following abbreviations:

$$\begin{aligned} h^2 &= (qL - N_dN_B\lambda\sin\xi')^2 + (N_dN_B\lambda\cos\xi')^2\\ \chi &= \tan^{-1}\left(\frac{qL - N_dN_B\lambda\sin\xi'}{N_dN_B\lambda\cos\xi'}\right). \end{aligned} \tag{34}$$

Further, in going to the last approximate equation in (33), we have neglected the variation of the logarithm with ζ, using the same approximation that led to a Gaussian scattering law for the $B = 0$ case. Since we are now primarily interested in the general behavior of the scattering, this approximation is adequate and it greatly simplifies the analysis.

The scattering is now quite different from the $B = 0$ case. Even though a closed-form solution for the final integral is not possible for all values of the variables, there are two ranges of important behavior, depending on the magnitude of qL relative to N_dN_B. When $qL \ll N_dN_B$, then $h^2 \to N_d^2N_B^2\lambda^2$ and

$$\langle I(q)\rangle \simeq 4/N_d^2N_B^2. \tag{35}$$

The second case is $qL \gg N_dN_B$ when $h^2 \to q^2L^2$. Then the integration is again possible, and takes the same form as in the $B = 0$ case above (in the Gaussian approximation):

$$\langle I(q)\rangle \simeq \{4/N_dN_B^2 \ln[\eta \ln(\eta)/(\ln 2)]\} \times \exp\{-q^2L^2/N_dN_B^2 \ln[\eta \ln(\eta)/(\ln 2)]\}. \tag{36}$$

These two equations thus yield a flat scattering around the Bragg peak out to a critical scattering vector, $q_c \simeq N_dN_B/L$. This critical q simply describes the 'bending' of the lattice generated by the screw dislocations. Around q_c, the scattering falls off abruptly and converges to the $B = 0$ solution.

The $B \neq 0$ case has been explored by Barabash, Krivoglaz & Ryaboshapka (1976) with equivalent results.

4. Computer simulations

As discussed in §2, scattering from a restrictedly random distribution of dislocations can be found by averaging the scattering intensities from many independent blocks. In the computer simulations, therefore, line profiles for many different blocks are calculated and then averaged. Each block simulation uses a different spatially uncorrelated arrangement of dislocations whose positions are determined using a random number generator. No approximations are made since we use (2) directly and evaluate the intensity by computing SS^*. The lattice sums were carried out for 2D circular samples with an underlying square lattice. Typically, $N_0 \simeq 10^4$. The results will be reported in terms of the size parameter, L, expressed in units of the lattice parameter, a_0.

Fig. 5 shows a contour plot of the 001 peak from a single circular diffracting region with $L = 50a_0$ and $N_d = 50$. The large fluctuations are typical of scattering from a spatially random collection of dislocations. Averaging a large number of such simulations together as described above results in a smooth circularly symmetric intensity distribution. We find that, as the size of a single simulation increases (with a constant dislocation density), the characteristic wavelength of the oscillations decreases. Thus, even if a sample contained just one macroscopic block, an instrument with a finite resolution would perceive only the local average value of the scattering. For practical purposes, therefore, the radius, L, of our computer simulations can be interpreted either as the size of a scattering block within a larger sample or as the size of a sample containing just one block. The same is true for our theoretical formalism.

Fig. 6 shows scattering results for three cases of randomly distributed screw dislocations in a circular lattice with $B = 0$. As discussed above, these plots are intensity averages of simulations from many individual blocks. Since the resulting scattering distributions must be circularly symmetric about the Bragg peak, we display just a single radial cross section. In each of the three plots, the solid curves are the theoretical predictions from (29) and the individual data points come from the computer simulations. Error bars have not been included on the points from the computer simulations since the size of the error is well approximated by the small fluctuations visible in these profiles. The parameters used in Fig. 6(*a*) are $L = 100a_0$ and $N_d = 100$; those for Fig. 6(*b*) are $L = 200a_0$ and $N_d = 500$. In both cases, the 001 peak is displayed. The theoretical predictions accurately follow the computer simulations in the tails of the distributions. At the peaks, we find nearly perfect

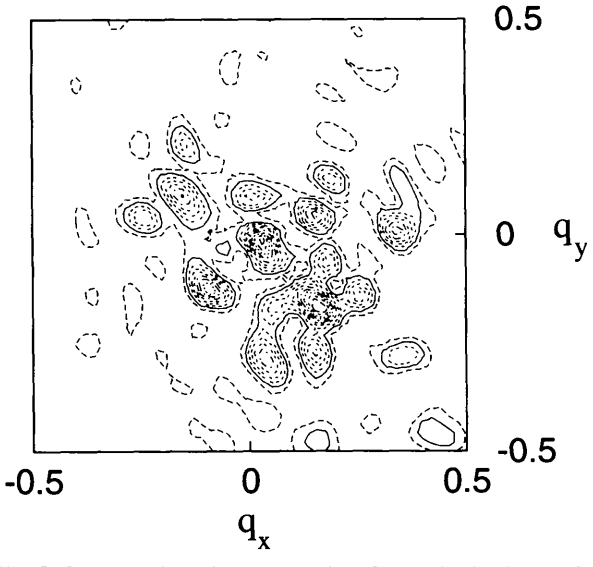

Fig. 5. Scattering intensity contour plot of a single simulation of a circular block containing 50 randomly positioned screw dislocations and with $L = 50a_0$ (a_0 is the lattice parameter). The contours are very tortuous and fluctuate strongly. When a large number of independent simulations are averaged, the fluctuations smooth out and the scattering becomes circularly symmetric. Here, q is expressed in units of $2\pi/a_0$.

agreement in Fig. 6(*b*) and only a small deviation in Fig. 6(*a*). Analysis of many such plots suggests that the theoretical predictions improve as the number of dislocations increases. This is not surprising since our expansion of $\langle A \rangle$ becomes more accurate as N_d increases. Fig. 6(*c*) shows a plot of the 002 peak with $L = 200a_0$ and $N_d = 500$. Although agreement is still quite good in the tails of the distribution, the overall fit is not as good as that observed in the previous simulations. Once again, agreement improves with increasing numbers of dislocations.

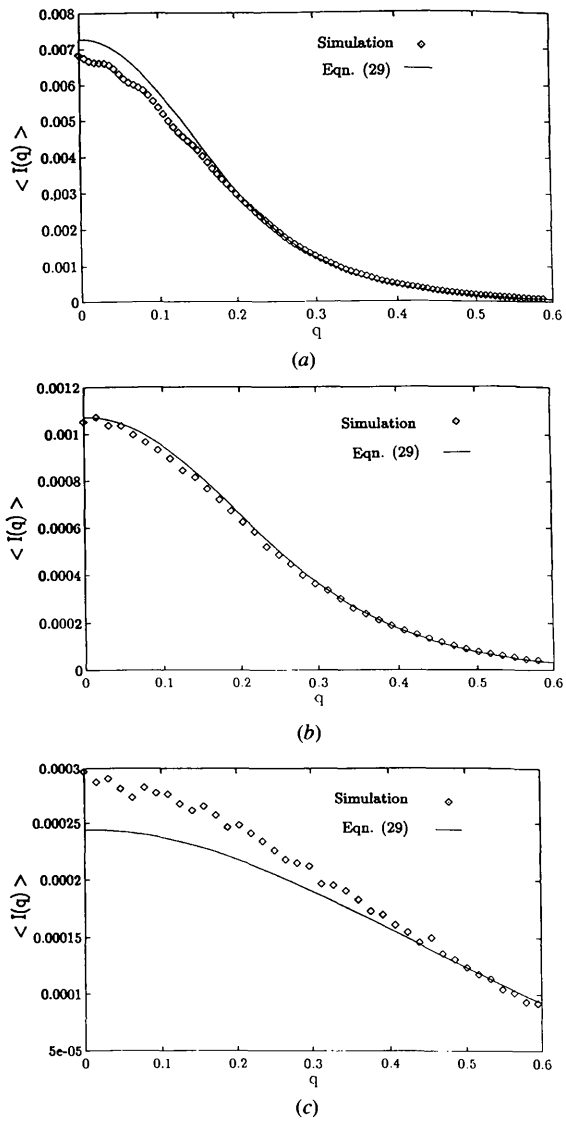

Fig. 6. Simulation results for a variety of cases with $B = 0$, compared with equation (29). Each case is averaged over a large number of separately randomized simulations. The data points represent the computer simulations and the full lines are the theoretical predictions from equation (29). In all cases, q is expressed in units of $2\pi/a_0$. (*a*) Scattering from a circle of radius $100a_0$, with 100 dislocations and averaged over 10 000 simulations. First Bragg peak, $N_B = 1$. (*b*) Scattering from a circle of radius $200a_0$, with 500 dislocations and averaged over 5000 simulations. First Bragg peak, $N_B = 1$. (*c*) Scattering from a circle of radius $200a_0$ with 500 dislocations and averaged over 5000 simulations. Second Bragg reflection, $N_B = 2$.

One final check that must be made concerns our prediction that $\langle I(0) \rangle$ [not $\langle I_a(0) \rangle$] is independent of the sample size, L. As shown by (31), we expect $\langle I(0) \rangle$ to depend only upon N_d and N_B. We have varied L in our simulations while keeping N_d constant and have found that $\langle I(0) \rangle$ is indeed independent of L.

The observed agreement between the theory and the simulations is remarkably good. We stress that there were no adjustable parameters in any of the plots. Of course, the agreement can only be investigated for sample sizes and dislocation densities that we can do in reasonable times on current work stations, and $L = 200a_0$ was the largest practical lattice for us. However, as remarked above, the quality of the theoretical prediction is likely to improve as the number of dislocations increases. We conclude that (29) accurately describes the scattering from screw dislocations with $B = 0$.

Fig. 7 shows the 001 peak for a circular sample of radius $50a_0$, with $N_d = 50$ and $B = 50$. Thus, all of the dislocations have the same Burgers vector. The scattering is approximately constant (though somewhat ragged due to the statistics) from $q = 0$ to a critical q_c, where a sharp fall-off takes place. As predicted in §3, $q_c \simeq N_d/L = 0.5$. This q_c corresponds quantitatively to the lattice 'rotation' induced by $B \neq 0$. (The actual lattice geometry is not a pure rotation, of course, because two sets of screws are necessary to cause pure rotation.)

5. Conclusions

In this paper, we develop a new approach to dislocation X-ray scattering theory based on a straightforward application of probability theory. In addition, we make central use of the proposition that, for large N, the Nth

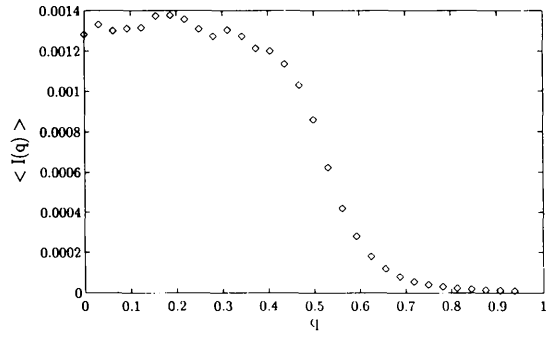

Fig. 7. Computer simulation of the scattering from a circle of radius $100a_0$ with 50 same-sign screw dislocations ($B = 50$) and averaged over 2000 simulations. As described in the text, the shape of this distribution matches the theoretical predictions.

power of a peaked function is very strongly peaked. An integral over the resulting function is accurately found by integrating the lowest-order expansion around the peak position. In our case, $N = N_d$ is the (large) number of dislocations. After developing the general equations, they are applied to the problem of scattering by screw dislocations in 2D. Analytically, the screw dislocation problem turns out to be barely tractable, provided a number of reasonable approximations are made. The results obtained, even in this simple case, highlight the physical features of dislocation scattering in general, and will be useful in guiding our approach to the more difficult edge dislocation scattering in a subsequent paper.

We have two principal conclusions. First, the scattering intensity of a (screw) dislocated crystal is non-Gaussian in form, and given very well by (29). Computer simulations indicate that the accuracy of this solution increases with increasing N_d. For the first Bragg peak, good convergence to (29) was demonstrated at $N_d \simeq 100$; for higher-order Bragg peaks, convergence appears to be slower. Second, in a sample with fixed dislocation density, as the block size goes to infinity, the lattice loses all scattering coherence. These conclusions are discussed in turn.

As expected from previous analyses of experimental results (Young & Wiles, 1982), (29) yields results that are 'intermediate' between Gaussian and Lorentzian distributions. (The results of Young & Wiles, being experimental, contained other contributions to the line broadening associated with instrumental factors *etc.*, which we cannot evaluate. But their non-Gaussian results are certainly in line with our predictions, suggesting that physical factors, as well as instrumental, may have been important. We are indebted to a reviewer for bringing up this point.) Deviation from a Gaussian solution arises from a proper estimate of the lower limit of the integral for $\langle a \rangle$. Unfortunately, this limit also leads to a final solution that can only be evaluated numerically.

Previous authors have made different choices for this lower limit. Krivoglaz and Ryaboshapka (Krivoglaz, 1996; Krivoglaz & Ryaboshapka, 1963) take a limit that is independent of the integration variable in our equation (29); as discussed in §3, this choice is inaccurate but it does allow them to obtain an approximate analytic solution that is a Gaussian distribution. In our own analysis, where the statistical treatment is more rigorous, if we take a lower limit that is proportional to the sample size, then we also arrive at a Gaussian line shape. There is good physical reasoning for such a choice as an approximation: $\langle a_2 \rangle$, because of its definition as a normalized volume average, must not scale with the sample size, a requirement that is possible if the lower limit is taken to be proportional to the sample size, L. This makes the argument of the logarithm term a constant and the final result is found to be roughly equivalent to Krivoglaz's approximate solution.

Wilkens (1970*a*,*b*), on the other hand, looks very hard at this lower limit. Working with what appears to be his equivalent of our amplitude function, A_g, he finds a very complicated function for our logarithm term, $\ln(\zeta_0/\zeta)$, in (29). In a later paper (Wilkens, 1970*b*), this function is greatly simplified to a logarithmic expression similar to our own, although several important differences in detail still remain.

Owing in part to errors in Wilkens's published geometric factors, we were unable to use his published solution to obtain physically realistic line shapes. Comparison between our basic definitions and those of Wilkens suggests that our differences lie in how we relate the functions A_g and $\langle A \rangle$ to the scattering intensity. This, in turn, suggests that the Wilkens function A_g should not be functionally equivalent to our amplitude function, $\langle A \rangle$. A final point of contact is his published curve [Fig. (2) in Wilkens, 1970*b*]. When we compare that figure with our numerical results as given in our Fig. 2, we seem to get a stronger deviation from the Gaussian than he reports. To summarize, we have been unable to use Wilkens's published equations to reproduce physically correct scattering profiles. Also, comparisons between his results and our solution, (29), show substantial differences in the respective functional forms.

We have also explored the asymptotic behavior of the scattering intensity. From (29), we find that the intensity varies as $\langle I(q) \rangle \propto 1/q^4$, which differs from both Krivoglaz's (1996) and Wilkens's predictions. Numerical integration of (29) was used to examine the q dependence at large, but finite, q. Some reasonable parameters gave a near-perfect agreement with Krivoglaz's q^{-5} prediction; other reasonable choices gave a near perfect agreement with our large-q prediction of q^{-4}. This variation suggests that the intensity converges so slowly to a power law that our simulations were not carried out at a sufficiently large q. Although there is some apparent uncertainty between the predictions of Krivoglaz and ourselves, we do not see the q^{-3} dependence reported by Wilkens (1970*b*).

All of the above results relate to the case $B = 0$. When $B \neq 0$, we find the peak is broadened by the lattice 'rotation' contributed by the dislocations in the crystal. For significant non-zero content, the peak becomes flattened on the top, with a sharp fall-off at a q value corresponding to the lattice rotation. In the Gaussian approximation we used for this case, the wings of the distribution follow the same behavior as predicted for the $B = 0$ case. This same result has previously been reported by Barabash *et al.* (1976).

The second major conclusion of the paper concerns the sample-size dependence of the scattering. Analysis of (29) shows that, for a fixed dislocation density, the maximum peak height per atom, $\langle I_a(0) \rangle$, decreases

approximately as $1/\ln(L)$. Since the integrated $\langle I_a(q)\rangle$ for a given Bragg peak must be constant as the sample size increases, there exists a reciprocal relation between peak height and peak width. Thus, as $\langle I_a(0)\rangle \to 0$ with increasing sample size, the width of the distribution must diverge and the sample loses all coherence.

The above functional dependence of the size scaling agrees roughly with both Krivoglaz's Gaussian analysis and Wilkens's report that the peak width is approximately proportional to $\ln(c^{1/2}L)$. This size scaling is a direct confirmation of Wilkens's basic thinking regarding the sample-size dependence of dislocation scattering. Thus, in any experimental measurement on a macroscopic dislocated sample, a finite peak width reflects the length scale beyond which the dislocations are not randomly distributed.

This leads us to a final question regarding the use of Wilkens's results for analyzing experimental data. In his interpretation of experimental results, Wilkens (1984) relies on the shape of the scattering function to determine his parameter, M, which is essentially our $(N_d/\pi)^{1/2}$. He then finds that M is always of the order 1! This implies that the block size is roughly equal to the distance between dislocations. This is a very remarkable result and we wonder if this is the correct interpretation, for several reasons. First, of course, is our difficulty in relating to his scattering intensity function, $I(S)$. More fundamentally, we believe that it is dangerous to use a functional form originally derived for screw dislocations to fit experimental data where edge dislocations predominate. Also, parameters such as peak heights, peak widths and asymptotic tails can be measured with some degree of confidence. The exact functional form of a curve, however, is likely to be much more sensitive to experimental and theoretical details. Therefore, we believe it may be more reasonable to base a measure of N_d on a comparison of peak heights with Bragg order, perhaps tempered by considerations of peak shape. But this is a point we wish to pursue only after we have presented the edge scattering results in a following paper.

In spite of the success we have demonstrated in our theoretical treatment of the above scattering problem, we must emphasize that a major issue of scattering from dislocations remains essentially unresolved. This involves the partially ordered nonrandom character of dislocation structures in physical systems. In Wilkens's original view (Wilkens, 1970*a*), nonrandomness is associated with the block size of his restrictedly random distribution. In Krivoglaz's (1996) view and in that of Groma *et al.* (1988), Ungar *et al.* (1989) and Gaal (1984), it is associated with the pair correlations in the distribution. Both of these viewpoints have merit, but neither approach answers the important question of what the measured coherence length really means in a physical system. At present, the most feasible approach to this problem would be through computer simulations of scattering from model systems, a problem to which we return in a later work.

APPENDIX *A*

In this section, we develop an asymptotic expansion for (29),

$$\langle I(q)\rangle = 2\int_0^{\zeta_0/3} J_0(q\zeta L)\exp\{[-N_d(N_B\zeta)^2/2]\ln(\zeta_0/\zeta)\}\zeta\,d\zeta$$
$$= (2/p^2)\int_0^{p\zeta_0/3} xJ_0(x) \times \exp\{[-N_dN_B^2x^2\ln(p\zeta_0/x)]/2p^2\}\,dx, \qquad (37)$$

where $x = p\zeta$ and $p = qL$. As $q \to \infty$, the exponential function and the integration limits spread out with respect to $xJ_0(x)$. We make the crucial assumption that when the oscillations in the Bessel function are very fast relative to the variation in the exponential, the only significant contribution to the integral comes where the magnitude of the argument of the exponential is much less than 1,

$$x \ll (p/N_B)[2/N_d\ln(p\zeta_0/x)]^{1/2}. \qquad (38)$$

If true, then the exponential can be expanded to give

$$\langle I(q)\rangle \simeq (2/p^2)\int_0^{x_{max}} xJ_0(x) \times \{1 - [N_dN_B^2x^2\ln(p\zeta_0/x)]/2p^2\}\,dx, \qquad (39)$$

where x_{max} satisfies the condition in (38). The only q dependence in the first integral in (39) is in the upper limit. Therefore, as $q \to \infty$, we can also let $x_{max} \to \infty$ in this first integral, which then becomes identically zero, leaving

$$\langle I(q)\rangle \simeq (N_dN_B^2/p^4)\int_0^{x_{max}} x^3J_0(x)[\ln(x) - \ln(p\zeta_0)]\,dx. \qquad (40)$$

We can now pull all of the q dependence out of the integrands, allowing us, once again, to set the upper integration limits to ∞. These integrals can also be evaluated exactly, giving

$$\langle I(q)\rangle \approx 4N_dN_B^2/p^4 = 4\pi N_B^2c/L^2q^4. \qquad (41)$$

In this last equation, we remember that $c = N_d/(\pi L^2)$ is the dislocation density.

Given the assumption that we can expand the exponential in (37), the asymptotic limit given by (41) is exact. We must emphasize, however, that the above analysis suggests a very complicated behavior for finite q. Therefore, it is not surprising that numerical integration of (29) for different values of N_d and L gives apparent power-law behaviors that wander between q^{-4} and q^{-5}. We note, however, that we

never find power-law behavior as low as q^{-3} as predicted by Wilkens (1970*b*).

References

Barabash, R. I., Krivoglaz, M. A. & Ryaboshapka, K. P. (1976). *Fiz. Metal. Metalloved.* **41**, 33–43.

Gaal, I. (1984). *Proceedings of the 5th Risø International Symposium on Metallurgy and Material Science*, edited by N. H. Anderson, M. Eldrup, N. Hansen, D. J. Jensen, T. Leffers, H. Lifhold, O. B. Pedersen & B. N. Singh, pp. 249–254. Denmark: Risø National Laboratory.

Groma, I., Ungar, T. & Wilkens, M. (1988). *J. Appl. Cryst.* **21**, 47–53.

Hirth, J. P. & Lothe, J. (1982). *Theory of Dislocations*. New York: Wiley.

Krivoglaz, M. A. (1996). *X-ray and Neutron Diffraction in Nonideal Crystals*. Berlin: Springer.

Krivoglaz, M. A. & Ryaboshapka, K. P. (1963). *Fiz. Metal. Metalloved.* **15**, 18–31. Engl. transl: *Phys. Metals Metallog.* (1963), **15**, 14–26.

Kuhlmann-Wilsdorf, D. (1995). *Scr. Mater.* **34**, 641–650.

Mugrabi, H., Ungar, T., Kienle, W. & Wilkens, M. (1986). *Philos. Mag.* A**53**, 793–813.

Ungar, T. & Borbeli, A. (1996). *Appl. Phys. Lett.* **69**, 3173.

Ungar, T., Groma, I. & Wilkens, M. (1989). *J. Appl. Cryst.* **22**, 26–34.

Warren, B. E. (1990). *X-ray Diffraction*. New York: Dover.

Wilkens, M. (1970*a*). *Fundamental Aspects of Dislocation Theory*, edited by J. A. Simmons, R. de Wit & R. Bullough, Vol. II. *Natl Bur. Stand. (US) Spec. Publ.* No. 317, pp. 1191–1193, 1195–1221.

Wilkens, M. (1970*b*). *Phys. Status Solidi A*, **2**, 359–370.

Wilkens, M. (1984). *Microstructural Characterization of Materials by Non-Microscopic Techniques*, edited by N. H. Anderson, M. Eldrup, N. Hansen, D. J. Jensen, T. Leffers, H. Lifholt, O. B. Pedersen & B. N. Singh, pp. 153–168. Denmark: Risø National Laboratory.

Young, R. A. & Wiles, D. B. (1982). *J. Appl. Cryst.* **15**, 430–438.